



Article

Synthesis of CuAl-, CoAl-, and CuCoAl-Catalysts from Layered Hydroxides for Furfural Hydrogenation

Liudmila N. Stepanova ^{1,*}, Roman M. Mironenko ¹ , Elena O. Kobzar ¹, Natalia N. Leont'eva ¹ ,
Tatiana I. Gulyaeva ¹, Anastasia V. Vasilevich ¹, Aleksandra N. Serkova ², Aleksei N. Salanov ²
and Aleksandr V. Lavrenov ¹

¹ Center of New Chemical Technologies BIC, Boreskov Institute of Catalysis, 644040 Omsk, Russia

² Department of Catalyst Investigation, Boreskov Institute of Catalysis, 5 Acad. Lavrentieva Ave., 630090 Novosibirsk, Russia

* Correspondence: lchem@yandex.ru

Abstract: Catalysts based on CuAl-, CoAl-, and CuCoAl-layered hydroxides with $M^{2+}/Al = 2$ and $Cu/Co = 1$ molar ratio were obtained. The effect of amount of cobalt on the structural properties, morphology, surface cations distribution, oxide phase formation, thermal stability of the samples and reduction of metals from them was studied. The effect of reaction conditions (temperature, time, pressure, solvent) and conditions of preliminary treatment of catalysts on their catalytic properties in furfural hydrogenation was established. High selectivity to furfuryl alcohol was observed for all the samples irrespective of pretreatment and reaction conditions. The synergetic effect in furfural hydrogenation between Co and Cu in the $CuCoAlO_x$ catalysts was revealed when ethanol is used as a solvent.

Keywords: layered hydroxides; copper; cobalt; furfural hydrogenation; TPR; SEM; TG/DTG/TA



Citation: Stepanova, L.N.;

Mironenko, R.M.; Kobzar, E.O.;

Leont'eva, N.N.; Gulyaeva, T.I.;

Vasilevich, A.V.; Serkova, A.N.;

Salanov, A.N.; Lavrenov, A.V.

Synthesis of CuAl-, CoAl-, and
CuCoAl-Catalysts from Layered
Hydroxides for Furfural

Hydrogenation. *Eng* **2022**, *3*, 400–411.

<https://doi.org/10.3390/eng3040029>

Academic Editors: George Z.

Papageorgiou, Maria Founti and

George N. Nikolaidis

Received: 24 August 2022

Accepted: 24 September 2022

Published: 28 September 2022

Publisher's Note: MDPI stays neutral with regard to jurisdictional claims in published maps and institutional affiliations.



Copyright: © 2022 by the authors. Licensee MDPI, Basel, Switzerland. This article is an open access article distributed under the terms and conditions of the Creative Commons Attribution (CC BY) license (<https://creativecommons.org/licenses/by/4.0/>).

1. Introduction

Layered double hydroxides (LDHs, hydrotalcite-like materials) are a class of inorganic compounds with general formula $[M(II)_{1-x}M(III)_x(OH)_2]^{x+} \times [A_{x/n}]^{x-} \times mH_2O$, where M(II) and M(III) are divalent and trivalent cations, A^{n-} is the anion, and x can generally have the values between 0.2 and 0.4 [1]. Structurally, LDHs are similar to a layered structure of brucite $Mg(OH)_2$, wherein partial substitution of bivalent metal ion (M(II)) by trivalent ion (M(III)) occurs. The resulting excess positive charge in the layers are compensated by anions (A^{n-}) that occupy in the interlayers along with water molecules. After LDH calcination in air at moderate temperature, mixed oxides with high specific surface area are formed [2]. The metal ions present a uniform dispersion at the atomic level in the LDHs layers. Thus, the metal species can still be well dispersed as a structure of corresponding mixed oxides. Owing to their flexible structural nature and ability to tune desired properties through facile synthetic or modification process LDHs and corresponding mixed oxides are extensively studied as catalysts for various organic reactions [3,4].

In recent years, much attention is paid to the development of new possibilities of fuel and chemicals production from no-fossil carbon resources. In this regard, the study of catalytic transformations of different biomass-derived compounds is of great interest. Furfural (FAL) is one of the most promising platform molecules directly derived from biomass. FAL implication routes to the manufacture of high volume products have a great interest. FAL hydrogenation allows for obtaining furfuryl alcohol (FOL), tetrahydrofurfuryl alcohol (THFOL), tetrahydrofurfural (THFAL), 2-methylfuran (2-MF), and 2-methyltetrahydrofuran (2-MTHF). These products can be used as intermediates for the preparation of different industrial valuable compounds. For example, FOL is a very important monomer for the synthesis of furan resins, which are widely used in thermoset polymer matrix composites, cements, adhesives, coatings, and casting/foundry resins. THFOL can be used as a green

solvent in the pharmaceutical industry and, in addition, it constitutes an outstanding intermediate to produce dihydropyran, pyridine, tetrahydrofuran, and pentane-1,5-diol [5–9]. In this respect, the development of new catalysts allowing the production of desirable products with high selectivity is very prospective.

FAL hydrogenation has been widely provided using different non-noble metal catalysts due to their low cost and comparable properties with noble metal catalysts [10–12]. Among them, Cu-based catalysts are widely studied for its accessibility and satisfactory hydrogenating selectivity. Introduction of another hydrogenating metal (Ni, Co, Fe) to this type of catalysts is an attractive approach because it opens new possibilities to tune the catalysts' properties [13–15]. Providing the high dispersion of active metals also still remains the main problem. Thus, the development of new catalysts based on non-noble metals with their high dispersion is an intensively evolved scientific area.

LDHs containing transition metal ions in the lattice are of potential interest since redox chemistry may be combined with structural and geometric features to obtain materials exhibiting desired properties. Moreover, redox properties of metal ions are significantly modified by matrix, concentration and the presence of co-cations associated with the system. Cu-containing LDHs as catalyst precursors for the FAL hydrogenation were used in some scientific works [16–18]. It was noticed by Shao et al. [16] that CuMgAl catalysts synthesized from LDHs had highly dispersed Cu particles and tunable basic sites. These materials showed good catalytic performances in hydrogenation of FAL to FOL and the subsequent hydrogenolysis of FOL to pentane-1,2-diol and pentane-1,5-diol. Data about studying of the Co- or CuCo-containing catalysts based on LDHs for the FAL hydrogenation are even fewer. At the same time, the synergetic effect between Cu and Co in catalysts based on the Cu and Co-containing LDHs was studied in various reactions [19–23]. A range of Cu/Co ratio for the optimal catalytic characteristics is different for each specific reaction. Until now, information about the distribution of cobalt and copper on the surface of the catalyst is contradictory [23,24]. Apparently, this largely depends on the method of LDH preparation, the amount of Co and Cu, and the conditions of high-temperature treatment of the catalysts before the reaction. Therefore, their complex study is an important task.

In this work, the catalysts based on the CuAl-, CoAl- and CuCoAl-LDHs were synthesized by coprecipitation. The effect of the catalyst composition on their structural properties, morphology, cations distribution on the surface, thermal properties, mixed oxide formation and metal reduction was studied. The genesis of catalysts was studied by changing the calcination and reduction conditions.

2. Materials and Methods

2.1. CuAl-, CoAl- and CuCoAl-LDHs Synthesis

LDHs were synthesized by a coprecipitation method [25]. A solution containing metal nitrates (concentration of 1 mol L^{-1}) gradually added to the solution of sodium carbonate (concentration of 1 mol L^{-1}) at a constant temperature of $60 \text{ }^\circ\text{C}$. To obtain CoAl-LDHs, pH 10 was maintained, while to synthesize CuAl- and CuCoAl-LDHs, pH was 9.5. After subsequent aging at $60 \text{ }^\circ\text{C}$ for 18 h, washing, filtration and drying, LDHs containing predominantly carbonate-anions in interlayer space were obtained. To produce CuAlO_x, CoAlO_x and CuCoAlO_x, the corresponding LDHs were calcined at $550 \text{ }^\circ\text{C}$ for 3 h. The M^{2+}/Al and Cu/Co molar ratios in obtained catalysts were 2 and 1, respectively. Before the testing in FAL hydrogenation, the samples were reduced in flowing hydrogen at 500 or $800 \text{ }^\circ\text{C}$ for 2 h. The reduced samples were designated as CoAl-Red, CuAl-Red and CuCoAl-Red.

2.2. Physicochemical Characterization of the Samples

Structure of the synthesized LDHs was studied by X-ray diffraction (XRD) on a D8 Advance (Bruker, Billerica, MA, USA) diffractometer using a Cu-K α source in the 2θ angular range from 5 to 80° . The scanning step was 0.02° , and the signal integration time was 5 s/step . The phase composition of samples was identified using the international

diffraction database ICDD PDF-2. Cell parameters c and a of the LDHs were determined by (003) and (110) peaks positions, and the crystallite sizes L_c and L_a were determined by the Scherrer equation.

The surface morphology of the samples was investigated by using scanning electron microscopy (SEM) on a JSM-6460 LV (JEOL, Tokyo, Japan) instrument equipped with the tungsten cathode and working at an accelerating voltage of 20 kV. Before each experiment, the samples were ground in an agate mortar and fixed on a conducting double-sided carbon Scotch tape. To prevent the re-charging effects, a conducting gold film was sputtered on the fixed samples. Prior to each experiment, the samples were evacuated in the microscope chamber for 15–20 min to remove volatile compounds from the surface, which could exert a detrimental effect on the secondary electron emission and thus deteriorate quality of the image. The qualitative and quantitative X-ray spectral microanalysis was performed using a special analytical attachment of an energy dispersive X-ray (EDX) spectrometer INCA Energy-350 (Oxford Instruments, Abingdon, UK) with an energy resolution of 127.37 eV at 5.895 keV (Mn) for recording X-ray quanta with an energy from 0.1 to 20 keV. The indicated spectrometer makes it possible to identify all elements from Be⁴ to U⁹² at a minimum content in the sample of ca. 0.1 wt%. The characteristic X-ray quanta emitted upon interaction of the probe electrons with atoms of the sample are recorded by the spectrometer to obtain a spectrum demonstrating the distribution of the amount of quanta versus their energy.

Thermal analysis (TG/DTA and DTG) was carried out using a DTG-60 (Shimadzu, Kyoto, Japan) instrument in the air atmosphere from room temperature to 700 °C at a heating rate of 10 °C min⁻¹.

The specific surface area of the samples (S_{sp}) was measured by one-pot nitrogen adsorption on a Sorbtometer (Katakon, Novosibirsk, Russia) analyzer.

The reducibility of Cu and Co species in the LDH structure was examined by temperature-programmed reduction (H₂-TPR) on an AutoChem II 2920 (Micromeritics, Norcross, GA, USA) chemisorption analyzer equipped with a thermal conductivity detector (TCD). The H₂-TPR experiments were carried out using a mixture of 10 vol% H₂ and argon (the flow rate of 30 cm³ min⁻¹) in a temperature range of 30–800 °C at a heating rate of 10 °C min⁻¹.

2.3. Catalyst Testing

Liquid-phase hydrogenation of FAL was performed in a Miniclave drive (Büchi AG, Flawil, Switzerland) batch-type reactor. The reaction vessel was loaded with 500 mg of preliminary reduced catalyst and a solution of FAL (5.0 cm³) in 100 cm³ of distilled water or aqueous ethyl alcohol (95%). The reactor was flushed with argon and hydrogen to remove air. Then, the reactor was heated to a temperature of 90 °C and simultaneously filled with hydrogen gas to a total pressure of 20 bar. The experiments were conducted under the indicated conditions and vigorous stirring at 1000 rpm for 1 or 5 h. After completion of the reaction and cooling, the aqueous phase was separated from the catalyst by filtering. The quantitative determination of the reaction products was carried out by gas chromatography (GC) on a GKh-1000 (Khromos, Moscow, Russia) instrument equipped with a flame ionization detector and a ValcoBond VB-Wax capillary column (60 m × 0.32 mm, polyethylene glycol, stationary phase thickness 0.50 µm).

3. Results and Discussion

3.1. Effect of the Samples Composition on Their Structural Characteristics and Oxide Phase Formation

Figure 1a displays XRD patterns for the as-synthesized CuAl-, CoAl- and CuCoAl-LDHs. As can be seen, in all cases, a single LDH phase was obtained [1]. Patterns demonstrate the formation of the hydrotalcite phase with visible reflections indexed to the lattice planes (003), (006), (012), (015), (018), (110) and (113). Copper content increased the peaks on XRD patterns, which became more narrow and intensive. This may be due to the increase of crystallinity of the samples as their copper content increases. The two peaks (110) and

(113) reflections were hard to recognize in CuAl-LDH. This is due to Jahn-Teller distortion of Cu^{2+} , which is usually found in LDH systems containing copper [19,24]. The formation of the additional phase with unidentified peaks at XRD patterns (for example, between 012 and 015) also may be associated with the low stability of Cu^{2+} ions in LDH phase due to the Jahn-Teller effect. The high background level in the X-ray diffraction patterns of Co-containing systems is explained by the fluorescence that occurs when the diffraction patterns are recorded on an X-ray tube with a copper anode.

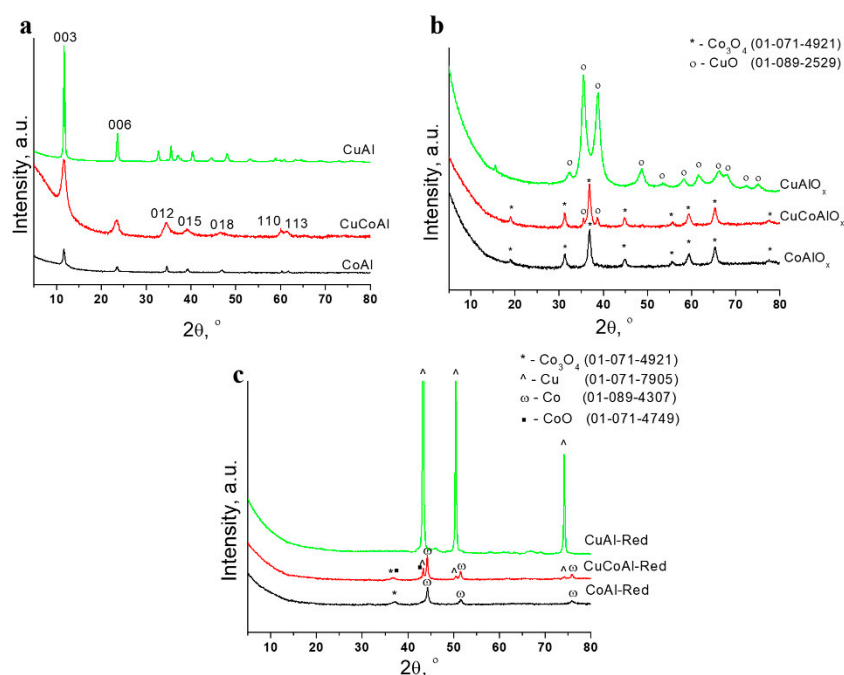


Figure 1. XDR patterns of the as-synthesized samples (a), samples, calcined at 550 °C (b), samples, calcined at 550 °C and then reduced at 800 °C (c). The intensity of CuAl peaks (for as-synthesized sample) was reduced by 10 times.

Lattice parameter a decreased with increasing cobalt content in the samples. This is due to the lower ionic radius of octahedrally coordinated Co^{2+} (0.65 Å) compared with Cu^{2+} (0.73 Å) in the same geometry environment [26]. CuAl-LDH was characterized by the smaller interlayer distance d_{003} and lattice parameter c compared with other samples. Probably, this is due to varied electrostatic interaction between layers. LDH containing both copper and cobalt in its composition was characterized by smaller crystallite sizes in the a and c directions (Table 1).

Table 1. Microstructural parameters of the CuAl-, CoAl- and CuCoAl-LDHs.

Sample	d_{003} , Å	c , Å	a , Å	L_c , Å	L_a , Å
CuAl	7.56	22.673	3.095	351	199
CuCoAl	7.60	22.802	3.081	81	195
CoAl	7.59	22.779	3.068	189	267

The phase composition of the systems obtained after calcination of CuAl-, CuCoAl- and CoAl-LDH has already been fairly well covered in the literature [21]. In our study, after calcination at 550 °C, the phases of CuO for CuAlO_x, CuO and CoAl oxide with mixed spinel structure for CuCoAlO_x, and CoAl oxide with mixed spinel structure for CoAlO_x was formed (Figure 1b). After reduction of mixed oxides, metallic coarse particles were formed for all the samples. The crystallite size of Cu was 57 nm in a CuAl-Red sample, the crystallite sizes of Cu and Co were 62 and 32 nm, respectively, in the CuCoAl-Red sample,

and the crystallite size of Co was 29 nm in the CoAl-Red sample. For CoAl-Red, except metallic Co, the CoAl mixed oxide with spinel structure is observed. For CuCoAl-Red, the mix of metallic phases (Co, Cu) and oxide phases (CoO, CoAl mixed oxide with spinel structure) are observed (Figure 1c).

The thermogravimetric (TG) curves, the corresponding differential (DTG) curves, and curves of differential thermal analysis (DTA) are shown in Figure 2. The total weight loss for the samples was almost the same: 35% for CuAl- and CoAl-LDHs and 32% for CuCoAl-LDH. However, the thermal behavior of CuAl-LDH differs from other samples. There is only one narrow and intense peak at the DTG-curve of CuAl-LDH with a maximum weight loss rate at 165 °C (Figure 2a).

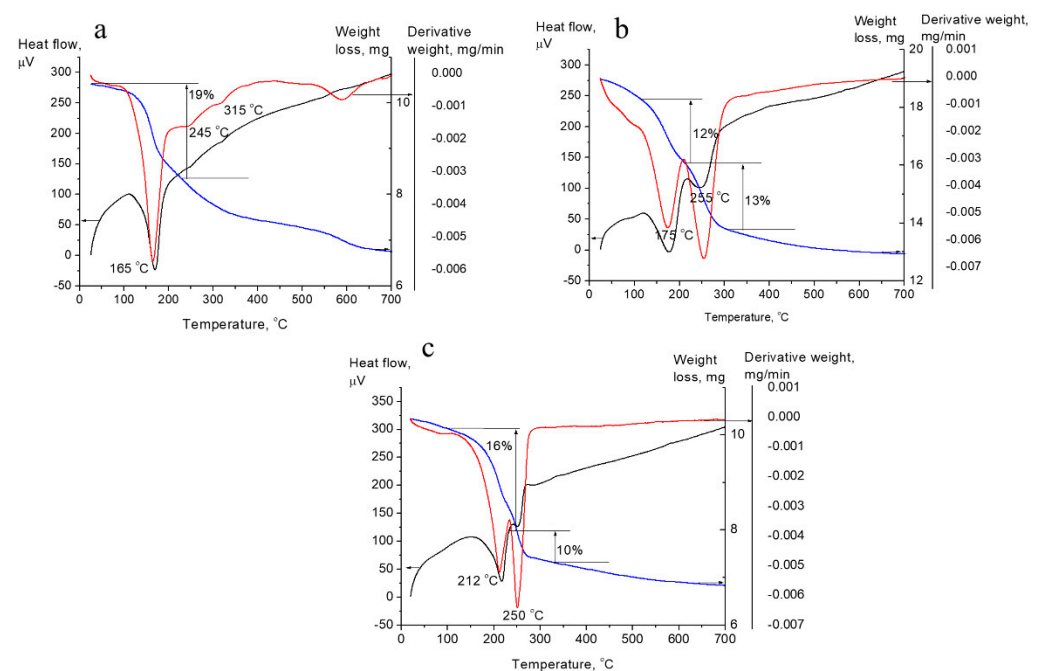


Figure 2. Curves of TG (blue line), DTG (red line), and DTA (black line) for the CuAl (a), CuCoAl (b), and CoAl (c) samples.

In this region, the greatest weight loss (19%) occurred. Minimum at a DTA-curve coincided with the minimum at a DTG-curve. Consequently, the weight loss in this temperature range was accompanied by a strong endothermic effect. CuCoAl- and CoAl-LDHs showed two different weight losses. The first weight loss for the CuCoAl-LDH was at 175 °C, and the second one at 255 °C (Figure 2b). The weight loss in this region was the same (12–13%). For CoAl-LDH, maximum weight loss was observed at 212 °C and 250 °C and corresponded to the 16 and 10% of total weight loss (Figure 2c). Narrower peaks for CoAl-LDH compared to CuCoAl-LDH corresponded to a faster decomposition process. According to DTA-curves for both CuCoAl-LDH and CoAl-LDH, the first weight loss was accompanied by a strong endothermic effect, while the second one by a much less thermal effect.

CuCoAl- and CoAl-LDHs showed the typical LDH thermal behavior. The first weight loss on DTG-curves corresponded to removal of interlayer water molecules. The second weight loss is usually attributed to dehydroxylation of brucite-like layers and decomposition of interlayer anions [27]. The presence of one intense peak for CuAl-LDH at low temperature indicates that these processes occurred almost simultaneously for this sample. This suggests the occurrence of the structural loss at a lower temperature for CuAl-LDH [23]. As Co content increased, the processes corresponding to these two stages (removal of interlayer water molecules and dehydroxylation of the layers with decomposition of interlayer anions) become more distinct. Herewith, the maximum of weight losses shifted to the high

temperature region. Thus, Co introduction into CuAl-LDH affected the formation of the oxide phase and contributed to the increase of thermal stability of the samples. Similar results were obtained by Rives et al. [19].

3.2. Study of the Surface Morphology of the Samples and Their Textural Characteristics

Changes of the surface morphology of CuAl-, CuCoAl- and CoAl-samples occurred after their high-temperature treatments (calcination at 550 °C, reduction of calcined samples at 800 °C) were studied by SEM. Moreover, chemical composition of the support surface was determined by EDX. Therewith, the chemical analysis by EDX can be made at certain points of the surface and in selected regions. A smooth surface of the sample is essential for the quantitative EDX microanalysis. Since most of the studied materials did not possess a perfectly smooth surface, this method was employed in a semiquantitative mode.

For as-prepared CuAl-LDH, rosette-like morphology is observed (Figure 3a). «Rosettes» are represented by platelets overlapping each other in different directions. CuCoAl-LDH areas with rosette-like morphology as well as smooth areas with sticky round plates are observed (Figure 3b). The morphology of CoAl-LDH is presented by small size platelets overlapping each other (Figure 3c). The high-temperature treatment of all the samples leads to the formation of their denser morphology. Herewith, the rosette-like morphology saved for the CuAl-samples after calcination and reduction steps. However, a reduction step leads to some conglutination of the CuAl platelets (Figure 3d,g). Reduction of mixed oxide CuCoAlO_x had a great effect on the surface morphology facilitating the transformation of the support consisting of disordered (randomly oriented) platelets in different directions to the smooth surface with dense packing of rounded particles (Figure 3e,h). The morphology of the calcined and reduced CoAl-samples remained always the same. They consisted of the platelets oriented mostly in the same plane (Figure 3f,i).

The increase of Co content in the samples led to the increase of their specific surface area (Table 2). Probably, it is due to more molecules in interlayer space of corresponding LDH (greater value of cell parameter *c* and significant amount of interlayer water according to DTG-curves) that form the pore structure of mixed oxides during calcination. A reduction step facilitated the decreasing of a specific surface area of all the samples. This is due to appearance of Co and Cu in the metallic form which are located in the pores and partially blocked them. The decrease of specific surface area of reduced samples is consistent with the formation of their denser morphology.

Table 2. M²⁺/Al and Co/Cu ratios calculated from energy dispersive analysis, as well as specific surface area of calcined (550 °C) and reduced (800 °C) samples.

Sample	M ²⁺ /Al, at. %	Co/Cu, at. %	S _{sp} , m ² g ⁻¹
CuAl	1.4–2.5	-	-
CuAlO _x	1.9–2.3	-	51
CuAl-Red	2.1–3.1	-	26
CuCoAl	3.1–3.8	3.1–3.6	-
CuCoAlO _x	3.1–5.9	2.0–3.3	65
CuCoAl-Red	5.3–7.5	3.6–3.9	37
CoAl	1.8–2.7	-	-
CoAlO _x	1.7–2.2	-	85
CoAl-Red	1.7–1.8	-	60

The surface ratios of Cu/Al and Co/Al evaluated from EDX in corresponding samples were close to the theoretical values calculated from the concentrations of solutions taking for the synthesis (Table 2). At the same time, CuAl-samples are characterized in a wider range of Cu/Al values compared to Co/Al range in CoAl samples. This is evidence of more uniform Co distribution on the surface of CoAl samples. On the surface of CuAl sample areas, low Cu (Cu/Al = 1.4) and high Cu (Cu/Al = 3.8) content existed.

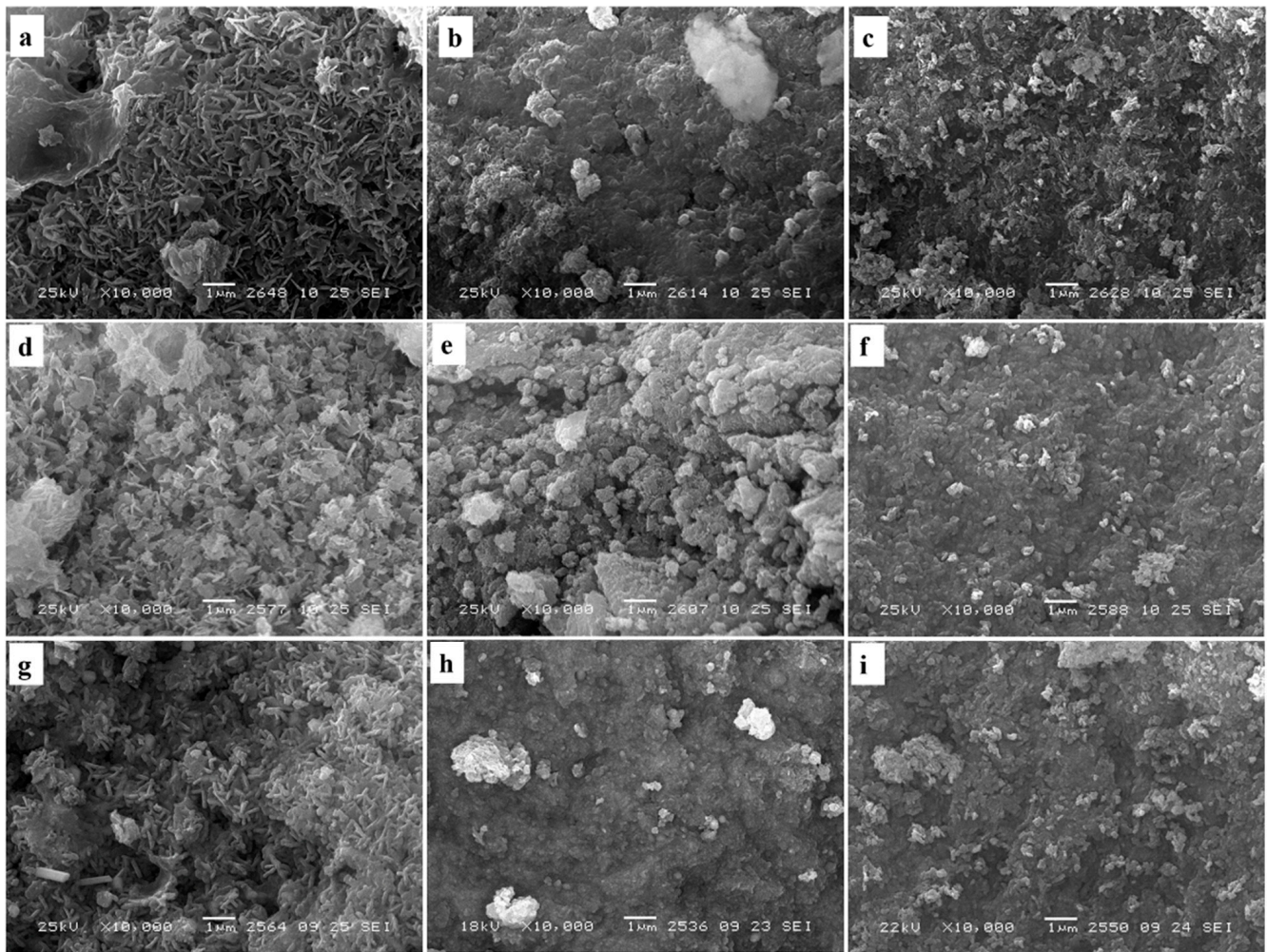


Figure 3. SEM images of CuAl (a,d,g), CuCoAl (b,e,h), and CoAl (c,f,i) samples in the forms of as-prepared LDHs (a–c), mixed oxides after calcination at 550 °C (d–f), and mixed oxides after reduction by hydrogen at 800 °C (g–i).

For the sample containing both Cu and Co metals, the M^{2+}/Al and Co/Cu ratios on the surface were much higher than theoretical values. After reduction, the surface was enriched in more extent by transition metals. Thus, the Cu present in the samples' composition facilitated easier Co exit from the bulk CuCoAl-LDH and its concentration on the sample surface.

3.3. Study of Metal Reduction from Mixed Oxides by H_2 -TPR

H_2 -TPR is a technique that allows for obtaining a knowledge about the reducibility of materials. H_2 -TPR is widely used to investigate LDHs with transition metal cations. In the case of CuAl- and CoAl-mixed oxides (derived after LDH calcination), the divalent cations (Cu^{2+} and Co^{2+}) were reduced to their metallic state while the trivalent cation (Al^{3+}) was unaffected in the temperature range studied.

H_2 -TPR profiles of $CuAlO_x$, $CuCoAlO_x$, and $CoAlO_x$ mixed oxides, obtained after calcination of corresponding LDH at 550 °C, are presented in Figure 4. The effects observed during the reduction of these systems can be explained from two positions: on the basis of the phase composition of the formed mixed oxides and on the basis of the size of the oxide particles formed after calcination.

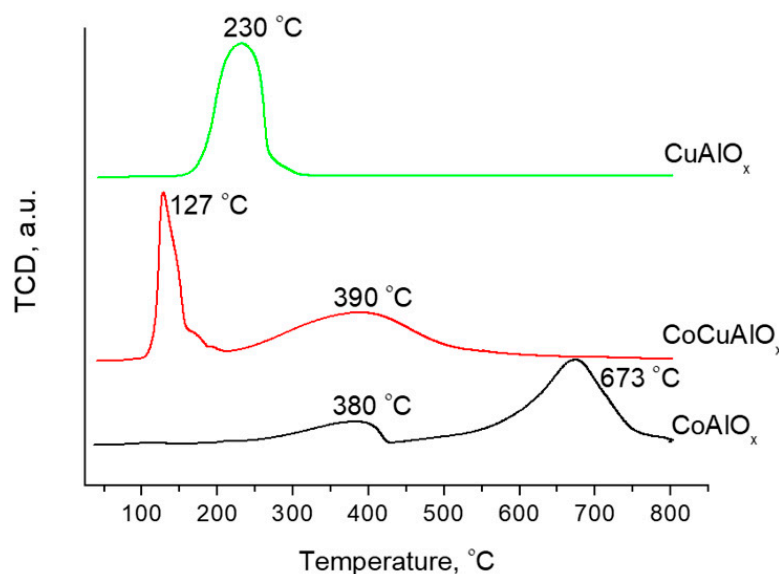


Figure 4. H₂-TPR profiles of the CuAlO_x, CuCoAlO_x and CoAlO_x.

A single broad peak with the maximum at about 230 °C was observed on H₂-TPR profile of CuAlO_x. It is well known that CuAl-LDH calcination of moderate temperatures (up to 700 °C) resulted in the formation of CuO/Al₂O₃ system [20]. Therefore, the single peak can be attributed to the reduction of copper (II) from corresponding oxide to metallic phase. According to XRD data (Figure 1c), a phase of metallic copper is present after reduction of CuAlO_x:



At the same time, individual copper oxide CuO has one broad reduction peak in the range of 300–350 °C on the H₂-TPR profile [24]. The lower reduction temperature of Cu²⁺ in the composition of LDH may indicate an increase in the dispersion of CuO oxide particles formed after the calcination of the CuAl hydroxide phase. The broadening of the peak can be due to the presence of several types of CuO species in the CuAlO_x composition, the reduction processes of which occur almost simultaneously: finely dispersed CuO species weakly bound to the Al₂O₃ surface and therefore more easily reduced, and more coarsely dispersed CuO particles reduced at a higher temperature.

Two distinct peaks in lower and higher temperature range appeared at H₂-TPR profiles with the increasing of cobalt content in the samples. The maxima of these peaks were shifted to the higher temperature when cobalt fraction in the catalysts increases.

The broad low intensity reduction peak with a maximum at about 380 °C and a more intense peak at 673 °C were observed for CoAlO_x. According to the literature data, both CoAlO_x and CuCoAlO_x have a complex and not fully understood phase composition [21].

Co₃O₄, CoAl₂O₄, Co^{II}Co^{III}AlO₄ and different types of non-stoichiometric Cu-Co spinels could form after CoAl-LDH calcination [19]. The peaks of these phases overlapped at XRD-patterns; therefore, it is difficult to make an unambiguous conclusion about the presence of one or another Co-containing phase. However, most researchers agree that the broad reduction peak at low temperature for CoAlO_x is associated with the simultaneous occurrence of cobalt reduction processes from Co₃O₄ and the weak interaction between Co₃O₄ and Al₂O₃:



The reduction peak at a higher temperature is due to the processes occurring during the reduction of cobalt from the CoAl spinel. It is known that the reduction of metals in such spinels is much more difficult [28]. At the same time, bulk Co₃O₄ also has two

reduction peaks on the H₂-TPR profile at 384 and 426 °C. The shift of the maxima of the hydrogen consumption peaks to a higher temperature region for CoAlO_x indicates an increase in the stability of Co when it is introduced into the composition of CoAl-LDH.

A low temperature peak at 127 °C on the H₂-TPR profile of CuCoAlO_x (with a small shoulder at 175 °C) most likely corresponds to the simultaneous reduction of Co₃O₄ to CoO and/or CuO to Cu⁰. The high intensity and sharpness of this peak may indicate a high dispersion of oxide species. The second reduction peak in a higher temperature region on the H₂-TPR profile of CuCoAlO_x may be due to the simultaneous reduction of CoO to Co⁰ and/or highly integrated Cu/Co oxide species reducing to the metallic state. At the same time, as noted by the authors of [21], the broadening of this peak can be due to two reasons: small amounts of spinel structures, which were more difficult to reduce, and/or the increased metal dispersion created small metal domains, which were harder to reduce.

Thus, the introduction of cobalt into the composition of LDH contributed to an increase in the stability of Co particles in a corresponding mixed CoAl oxide formed after CoAl-LDH calcination (compared to bulk Co₃O₄). At the same time, the presence of copper in the composition of CuCoAlO_x led to an improvement in the reducibility of Co. It is known that copper oxide has a tendency to be reduced. This, in turn, can lead to the hydrogen spillover effect, which facilitates the reduction of Co [21,23].

3.4. Catalytic Properties of the Samples in FAL Hydrogenation

The complexity of the phase composition of systems based on Cu- and Co-containing LDHs, which contributes to the formation of diverse metal species after appropriate thermal treatments, which can act as catalytically active sites, opens up great opportunities for targeted control of the properties of such catalytic systems by changing the pretreatment conditions and reaction conditions of selective hydrogenation of FAL. In the study of the genesis of catalysts based on CuAl-, CuCoAl-, and CoAl-LDH, their properties were studied by changing the calcination and reduction conditions, as well as the reaction conditions.

The properties of CuAl-, CuCoAl- and CoAl-LDH calcined at 550 °C and reduced at 800 °C were studied in FAL hydrogenation at 90 °C and 20 bar with the use of water or ethanol as a solvent. The calcination temperature was chosen in accordance with the thermal analysis data, according to which the layered structure was completely destroyed for all selected systems. In accordance with the H₂-TPR, the reduction of CoAl oxides ends at a temperature of 800 °C. For pretreatment identity, this reduction temperature was used for all samples. Moreover, in some experiments, CuCoAl-catalysts were reduced at 500 °C.

As can be seen from Table 3, the FAL conversion increased with the increase of Co content and reached 89% for CoAlO_x when water was used as a solvent. For CuAlO_x, the FAL conversion was negligible and did not exceed 1%. At the same time, high selectivity to FOL (>99%) was achieved for a CuCo-catalyst. A pronounced synergistic effect between Cu and Co in the catalysts based on CuCoAl-LDH was found when ethanol was used as a solvent. FAL conversion after 1 h of the reaction over this catalyst exceeded three times the same parameter for CoAlO_x and more than six times for CuAlO_x. In this case, in addition to FOL, furylethyl ether (FEE) was formed. Increase of the reaction time (5 h) for CoAlO_x and CuCoAlO_x (in H₂O and EtOH) facilitated the large increase of FAL conversion. Herewith, the best results were obtained for CuCoAlO_x in EtOH. For this sample, complete FAL conversion and the highest yield of FOL (98%) were achieved.

In addition, the effect of the calcination stage, reduction temperature and reaction conditions on catalytic properties was studied for the CuCoAlO_x catalyst. The reduction temperature was chosen in accordance with H₂-TPR data and corresponded to a different reduction degree of the metals in the sample. The exclusion of the calcination stage for these systems usually improves the reducibility of metals, although it can lead to deterioration in their dispersion [24]. The obtained catalytic results are presented in Table 4.

Table 3. Results of FAL hydrogenation in the presence of CuAl- CoAl- and CuCoAl-catalysts in the water and ethanol media.

Catalyst ^a	Solvent in FAL Hydrogenation ^b	Reaction Time, h	FAL Conversion, mol.% ^c	Yield of FOL, mol.% ^c	Selectivity to FOL, mol.% ^c
CuAlO _x ^d	H ₂ O	1	1	<1	44
CoAlO _x ^e	H ₂ O	1	89	87	98
CoAlO _x ^e	H ₂ O	5	>99	96	96
CuCoAlO _x ^f	H ₂ O	1	32	32	>99
CuCoAlO _x ^f	H ₂ O	5	81	81	>99
CuAlO _x ^d	EtOH	1	3	<1	<1
CoAlO _x ^e	EtOH	1	6	4	67
CoAlO _x ^e	EtOH	5	97	94	97
CuCoAlO _x ^f	EtOH	1	19	16	84
CuCoAlO _x ^f	EtOH	5	>99	98	98

^a Pretreatment conditions: calcination at 550 °C in air, reduction at 800 °C in H₂. ^b Reaction conditions: 90 °C, 20 bar. ^c According to GC. ^d Cu/Al = 2. ^e Co/Al = 2. ^f (Co + Cu)/Al = 2, Co/Cu = 1.

Table 4. Effect of pretreatment of CuCoAl-catalysts with atomic ratios (Co + Cu)/Al = 2 and Co/Cu = 1 on their performance in FAL hydrogenation at 90 °C, 20 bar for 1 h.

Entry	Pretreatment Conditions	FAL Conversion, mol.% ^a	Yield of FOL, mol.% ^a	Selectivity to FOL, mol.% ^a
1	Calcination at 550 °C in air, reduction at 800 °C in H ₂	32	32	>99
2	Calcination at 550 °C in air, reduction at 500 °C in H ₂	27	26	96
3	Calcination at 550 °C in air, reduction at 500 °C in H ₂	37 ^b	31 ^b	84 ^b
4	Reduction at 500 °C in H ₂ , without calcination	21	20	95
5	Reduction at 800 °C in H ₂ , without calcination	17	17	>99

^a According to GC. ^b At 150 °C, 30 bar, 1 h.

According to the data of Table 4, high selectivity to FOL was observed for all the samples irrespective of the pretreatment conditions. The best results were obtained for the systems that were preliminarily calcined and reduced at a high (800 °C) temperature. This can be due to a higher amount of metals reduced at this temperature. A broad peak at 390 °C on the H₂-TPR profile of CuCoAlO_x indicates a slow and incomplete reduction of metals at this temperature. This is why the reduction at lower temperatures (500 °C) did not lead to an increase in activity. According to the literature data, the absence of the calcination stage contributes to a decrease in the sample reduction temperature [23]. However, on the other hand, a broad peak on the H₂-TPR profile of this sample indicates an incomplete reduction. An increase in the reduction temperature up to 800 °C for the sample obtained without a preliminary calcination step should have contributed to an increase in the amount of the metal phase in the catalysts. However, most likely, it led to sintering of particles at such a high temperature and a decrease in catalyst activity. The study of CuCoAlO_x catalysts under more severe reaction conditions (increased temperature and pressure) contributed to an increase of FAL conversion but led to a decrease in the yield of FOL.

4. Conclusions

In the study, the CuAl-, CoAl- and CuCoAl-layered hydroxides with M²⁺/Al = 2 and Cu/Co = 1 molar ratios were synthesized by coprecipitation. According to XRD data,

the phase composition of obtained samples corresponds to hydrotalcite. It was shown by thermal analysis that an increase of cobalt content in the samples changes their thermal behavior. Decomposition of the CuAl-LDH occurs in one stage with a maximum rate of weight loss at 165 °C, while a cobalt introduction leads to the two-stage decomposition of the samples in the low temperature range (175–212 °C) and higher temperature range (250–255 °C). Thus, the temperature stability of the samples increases with the increase of Co content. An increase of Co content in the samples led to the increase of a specific surface area both after calcination and reduction treatments. In addition, according to SEM-EDX, CoAl-samples are characterized by a more uniform surface Co distribution. In accordance with H₂-TPR, the amount of copper strongly influences cobalt reduction in calcined LDH. Copper reduction from CuAlO_x occurs in a single stage with a maximum at 230 °C in H₂-TPR profile. Cobalt reduction from CoAlO_x occurs in two stages at 380 and 673 °C. Reduction of metal-oxide species in CuCoAlO_x was easier. There are two maxima at lower temperatures of 127 and 390 °C in the H₂-TPR profile of this sample.

High selectivity to furfuryl alcohol during furfural hydrogenation was achieved for all studied samples irrespective of the pretreatment and reaction conditions. The best catalytic characteristics after 1 h of reaction (furfural conversion 89%) were observed for the CoAlO_x with the use of water as the solvent. When ethanol was employed as a solvent, furfural conversion after 1 h of the reaction over CuCoAlO_x exceeded three times the same parameter for CoAlO_x and more than six times for CuAlO_x. Thus, the synergetic effect between Cu and Co in the CuCoAlO_x catalyst was apparently observed when the ethanol is used as a solvent in furfural hydrogenation. After 5 h of reaction, the best catalytic results were obtained for CuCoAlO_x in EtOH (FAL conversion >99%, yield of FOL 98%). In the next work, we are planning to study in detail the properties of active centers of the catalysts based on the CuAl-, CoAl- and CuCoAl-LDHs and the study of the kinetics of the reaction in the presence of these samples.

Author Contributions: L.N.S.—Conceptualization, Writing—original draft, Writing—review and editing; R.M.M.—Investigation, Writing—original draft, Writing—review and editing; E.O.K.—Investigation; N.N.L.—Investigation; T.I.G.—Investigation; A.V.V.—Investigation; A.N.S. (Aleksandra N. Serkova)—Investigation; A.N.S. (Aleksei N. Salanov)—Investigation; A.V.L.—Supervision. All authors have read and agreed to the published version of the manuscript.

Funding: This research was funded by Russian Science Foundation, Grant No. 22-23-20040, <https://rscf.ru/en/project/22-23-20040/>, and a grant in the form of a subsidy provided from the budget of the Omsk region.

Data Availability Statement: Data are contained within the article.

Acknowledgments: The authors are grateful to I.V. Muromtsev for the XRD experiments and G.G. Savel'eva for one-pot nitrogen adsorption. The research was performed using equipment of the Shared-Use Center "National Center for the Study of Catalysts" at the Boreskov Institute of Catalysis.

Conflicts of Interest: The authors declare no conflict of interest.

References

1. Cavani, F.; Trifiro, F.; Vaccari, A. Hydrotalcite-type anionic clays: Preparation, properties and applications. *Catal. Today* **1991**, *11*, 173–301. [[CrossRef](#)]
2. Balsamo, N.; Mendieta, S.; Oliva, M.; Eimer, G.; Crivello, M. Synthesis and characterization of metal mixed oxides from layered double hydroxides. *Procedia Mater. Sci.* **2012**, *1*, 506–513. [[CrossRef](#)]
3. Xu, M.; Wei, M. Layered double hydroxide-based catalysts: Recent advances in preparation, structure, and applications. *Adv. Funct. Mater.* **2018**, *28*, 1802943. [[CrossRef](#)]
4. He, S.; An, Z.; Wei, M.; Evans, D.G.; Duan, X. Layered double hydroxide-based catalysts: Nanostructure design and catalytic performance. *Chem. Commun.* **2013**, *49*, 5912–5920. [[CrossRef](#)]
5. Wang, Y.; Zhao, D.; Rodríguez-Padrón, D.; Len, C. Recent advances in catalytic hydrogenation of furfural. *Catalysts* **2019**, *9*, 796. [[CrossRef](#)]

6. Vargas-Hernández, D.; Rubio-Caballero, J.M.; Santamaría-González, J.; Moreno-Tost, R.; Mérida-Robles, J.M.; Pérez-Cruz, M.A.; Jiménez-López, A.; Hernández-Huesca, R.; Maireles-Torres, P. Furfuryl alcohol from furfural hydrogenation over copper supported on SBA-15 silica catalysts. *J. Mol. Catal. A Chem.* **2014**, *383–384*, 106–113. [[CrossRef](#)]
7. Taylor, M.J.; Durndell, L.J.; Isaacs, M.A.; Parlett, C.M.A.; Wilson, K.; Lee, A.F.; Kyriakou, G. Highly selective hydrogenation of furfural over supported Pt nanoparticles under mild conditions. *Appl. Catal. B* **2016**, *180*, 580–585. [[CrossRef](#)]
8. Sitthisa, S.; Sooknoi, T.; Ma, Y.; Balbuena, P.B.; Resasco, D.E. Kinetics and mechanism of hydrogenation of furfural on Cu/SiO₂ catalysts. *J. Catal.* **2011**, *277*, 1–13. [[CrossRef](#)]
9. Sato, S.; Igarashi, J.; Yamada, Y. Stable vapor-phase conversion of tetrahydrofurfuryl alcohol into 3, 4-2H-dihydropyran. *Appl. Catal. A* **2013**, *453*, 213–218. [[CrossRef](#)]
10. Meng, X.; Yang, Y.; Chen, L.; Xu, M.; Zhang, X.; Wei, M. A Control over hydrogenation selectivity of furfural via tuning exposed facet of Ni catalysts. *ACS Catal.* **2019**, *9*, 4226–4235. [[CrossRef](#)]
11. Shi, D.; Yang, Q.; Peterson, C.; Lamic-Humblot, A.-F.; Girardon, J.-S.; Griboval-Constant, A.; Stievano, L.; Sougrati, M.T.; Briois, V.; Bagot, P.A.J.; et al. Bimetallic Fe-Ni/SiO₂ catalysts for furfural hydrogenation: Identification of the interplay between Fe and Ni during deposition-precipitation and thermal treatments. *Catal. Today* **2019**, *334*, 162–172. [[CrossRef](#)]
12. Villaverde, M.M.; Bertero, N.M.; Garetto, T.F.; Marchi, A.J. Selective liquid-phase hydrogenation of furfural to furfuryl alcohol over Cu-based catalysts. *Catal. Today* **2013**, *213*, 87–92. [[CrossRef](#)]
13. Manikandan, M.; Venugopal, A.K.; Nagpure, A.S.; Chilukuri, S.; Raja, T. Promotional effect of Fe on the performance of supported Cu catalyst for ambient pressure hydrogenation of furfural. *RSC Adv.* **2016**, *6*, 3888–3898. [[CrossRef](#)]
14. Seemala, B.; Cai, C.M.; Kumar, R.; Wyman, C.E.; Christopher, P. Effects of Cu–Ni bimetallic catalyst composition and support on activity, selectivity, and stability for furfural conversion to 2-methylfuran. *ACS Sustain. Chem. Eng.* **2018**, *6*, 2152–2161. [[CrossRef](#)]
15. Wang, Y.; Miao, Y.; Li, S.; Gao, L.; Xiao, G. Metal-organic frameworks derived bimetallic Cu-Co catalyst for efficient and selective hydrogenation of biomass-derived furfural to furfuryl alcohol. *Mol. Catal.* **2017**, *436*, 128–137. [[CrossRef](#)]
16. Shao, Y.; Wang, J.; Du, H.; Sun, K.; Zhang, Z.; Zhang, L.; Li, Q.; Zhang, S.; Liu, Q.; Hu, X. Importance of magnesium in Cu-based catalysts for selective conversion of biomass-derived furan compounds to diols. *ACS Sustain. Chem. Eng.* **2020**, *8*, 5217–5228. [[CrossRef](#)]
17. Prakruthi, H.R.; Chandrashekar, B.M.; Jai Prakash, B.S.; Bhat, Y.S. Hydrogenation efficiency of highly porous Cu-Al oxides derived from dealuminated LDH in the conversion of furfural to furfuryl alcohol. *J. Ind. Eng. Chem.* **2018**, *62*, 96–105. [[CrossRef](#)]
18. Fu, X.; Ren, X.; Shen, J.; Jiang, Y.; Wang, Y.; Orooji, Y.; Xu, W.; Liang, J. Synergistic catalytic hydrogenation of furfural to 1,2-pentanediol and 1,5-pentanediol with LDO derived from CuMgAl hydrotalcite. *Mol. Catal.* **2021**, *499*, 111298. [[CrossRef](#)]
19. Rives, V.; Dubey, A.; Kannan, S. Synthesis, characterization and catalytic hydroxylation of phenol over CuCoAl ternary hydrotalcites. *Phys. Chem. Chem. Phys.* **2001**, *3*, 4826–4836. [[CrossRef](#)]
20. Sun, K.; Gao, X.; Bai, Y.; Tan, M.; Yanga, G.; Tan, Y. Synergetic catalysis of bimetallic copper–cobalt nanosheets for direct synthesis of ethanol and higher alcohols from syngas. *Catal. Sci. Technol.* **2018**, *8*, 3936–3947. [[CrossRef](#)]
21. Sulmonetti, T.; Hu, B.; Lee, S.; Agrawal, P.K.; Jones, C.W. Reduced Cu-Co-Al mixed metal oxides for the ring-opening of furfuryl alcohol to produce renewable diols. *ACS Sustain. Chem. Eng.* **2017**, *5*, 8959–8969. [[CrossRef](#)]
22. Pan, K.; Yu, F.; Liu, Z.; Zhou, X.; Sun, R.; Li, W.; Zhao, H.; Liu, M.; Guo, X.; Dai, B. Enhanced low-temperature CO-SCR denitration performance and mechanism of two-dimensional CuCoAl layered double oxide. *J. Environ. Chem. Eng.* **2022**, *10*, 108030. [[CrossRef](#)]
23. Sankaranarayanan, S.; Sharma, A.; Srinivasan, K. CoCuAl layered double hydroxides—Efficient solid catalysts for the preparation of industrially important fatty epoxides. *Catal. Sci. Technol.* **2015**, *5*, 1187–1197. [[CrossRef](#)]
24. Akil, J.; Ciotonea, C.; Siffert, S.; Royer, S.; Pirault-Roy, L.; Cousin, R.; Poupin, C. NO reduction by CO under oxidative conditions over CoCuAl mixed oxides derived from hydrotalcite-like compounds: Effect of water. *Catal. Today* **2022**, *384–386*, 97–105. [[CrossRef](#)]
25. Miata, S. The syntheses of hydrotalcite-like compounds and their structures and physicochemical properties. I: The systems Mg²⁺-Al³⁺-NO₃⁻, Mg²⁺-Al³⁺-Cl⁻, Ni²⁺-Al³⁺-Cl⁻, Zn²⁺-Al³⁺-Cl⁻. *Clays Clay Miner.* **1975**, *23*, 363–375. [[CrossRef](#)]
26. Shannon, R.D. Revised effective ionic radii and systematic studies of interatomic distances in halides and chalcogenides. *Acta Crystallogr.* **1976**, *A32*, 751–767. [[CrossRef](#)]
27. Rives, V. Comment on “Direct observation of a metastable solid phase of Mg/Al/CO₃-layered double hydroxide by means of high-temperature in situ powder XRD and DTA/TG”. *Inorg. Chem.* **1999**, *38*, 406–407. [[CrossRef](#)]
28. Ribet, S.; Tichit, D.; Coq, B.; Ducourant, B.; Morato, F. Synthesis and activation of Co–Mg–Al layered double hydroxides. *J. Solid State Chem.* **1999**, *142*, 382–392. [[CrossRef](#)]